SIAM J. MATH. ANAL.
Vol. 24, No. 2, pp. 520-527, March 1993

015

ORTHONORMAL BASES OF COMPACTLY SUPPORTED WAVELETS III. BETTER FREQUENCY RESOLUTION*

A. COHEN† AND INGRID DAUBECHIES‡

Abstract. Standard orthonormal bases of wavelets with dilation factor 2 use wavelets with one octave bandwidth. Orthonormal bases with $\frac{1}{2}$ octave or even smaller bandwidth wavelets are constructed. These wavelets are special cases of the "wavelet packet" construction by R. Coifman and Y. Meyer [Yale University, preprint, 1990].

Key words. wavelets, orthonormal bases, frequency resolution

AMS(MOS) subject classifications. 26A16, 26A18, 26A27, 39B12

1. Introduction. In the preceding paper [1] one of us showed how to construct variations to [2] in order to obtain orthonormal bases of compactly supported wavelets with various desirable properties. In this paper we show how to construct orthonormal bases with better frequency localization.

We shall continue to use here the notation and terminology given in [1, § 1]. When we need equation (1.n) in [1], we shall refer to it as [1, (1.n)].

2. Statement of the problem. The Fourier transform $\hat{\psi}$ and ψ for an orthonormal wavelet basis of type [1, (1.1)] is, in most cases of practical interest, concentrated around a frequency band $a \leqq |\omega| \leqq 2a$. This "concentration" should be understood more or less loosely, depending on the example. For the Meyer basis [3], where $\hat{\psi}$ has compact support, we find support $(\hat{\psi}) \subset \{\omega;\ \pi - \varepsilon \leqq |\omega| \leqq 2\pi + 2\varepsilon\}$ for some $\varepsilon \in]0, \pi/3]$ (the "standard" choice is $\varepsilon = \pi/3$). For the functions constructed in [2], support$(\hat{\psi}) = \mathbb{R}$ (since support(ψ) is compact), but graphs of $\hat{\psi}$ show a reasonably good concentration around $\pi \leqq |\omega| \leqq 2\pi$ (see Fig. 7 in [2]).

It is the use of the dilation factor 2 in the definition [1, (1.1)] of the orthonormal basis that forces ψ to have a bandwidth of at least one octave. In many applications, especially those where a stationary high frequency component can be present (texture in images, music in acoustical signal analysis), it is desirable to have better frequency localization [4]. We present several approaches to the construction of such bases.

3. Noninteger dilation factors. Since the one-octave bandwidth is forced by the use of powers of 2, a natural way to obtain smaller bandwidth is to use a smaller dilation factor, e.g., $\frac{3}{2}$. There do indeed exist orthonormal wavelet bases for noninteger rational dilation factors α (for $\alpha = (k+1)/k$, $k \in \mathbb{N}$ this is an extension of Meyer's construction proposed by David [3]; for $\alpha = p/q$, a construction method is given in Auscher's Ph.D. thesis [5]). Unfortunately, these cannot correspond to a multiresolution analysis with compactly supported ϕ and ψ. For $\alpha = \frac{3}{2}$, e.g., $V_0 \subset V_{-1}$ implies the

* Received by the editors May 29, 1990; accepted for publication (in revised form) May 23, 1992.

† Centre de la Recherche de Mathematique de la Decision, Université Paris IX Dauphine, 75016 Paris, France.

‡ Mathematics Department, Rutgers University, New Brunswick, New Jersey 08903, and AT&T Bell Laboratories, 600 Mountain Avenue, Murray Hill, New Jersey 07974. Part of this author's work was done while visiting the University of Paris IX, Paris-Dauphine.

existence of two sequences, $(c_{1,n})_{n\in\mathbb{Z}}$ and $(c_{2,n})_{n\in\mathbb{Z}}$, such that

$$\text{(1)}\qquad \begin{aligned}\phi(x)&=\sum_n c_{1,n}\phi\left(\frac{3}{2}x-n\right),\\ \phi(x-1)&=\sum_n c_{2,n}\phi\left(\frac{3}{2}x-n\right).\end{aligned}$$

If ϕ were compactly supported, then both sequences would be finite. But (1) can be rewritten as

$$\frac{3}{2}\hat{\phi}\left(\frac{3}{2}\xi\right)=\left(\sum_n c_{1,n}\,e^{in\xi}\right)\hat{\phi}(\xi),$$

$$\frac{3}{2}e^{i3\xi/2}\hat{\phi}\left(\frac{3}{2}\xi\right)=\left(\sum_n c_{2,n}\,e^{in\xi}\right)\hat{\phi}(\xi),$$

implying

$$\sum_n c_{1,n}\,e^{in\xi}=e^{i3\xi/2}\sum_n c_{2,n}\,e^{in\xi},$$

which is impossible for finite sequences. The same phenomenon occurs for any noninteger α.

In practical applications, it is desirable to have finite sequences c_n for the hierarchic decomposition + reconstruction scheme sketched in [1, § 1]. We can, of course, always use truncated versions of infinite sequences, but untruncated finite sequences are preferable. Therefore, noninteger α does not seem to be a good solution. (Note, however, that Kovačević and Vetterli [10] have constructed subband filtering schemes with FIR filters and rational noninteger dilation factors; these do not correspond to a multiresolution analysis with a single ϕ.)

4. Integer dilation factors larger than 2. Another candidate for wavelet bases with better frequency localization is given by constructions with a dilation factor *larger* than 2. In general, a multiresolution scheme with dilation factor N uses one scaling function ϕ, and $N-1$ different wavelets ψ^l, $l=1,\ldots,N-1$ [5]. The function ϕ satisfies an equation of type [1, eqn. (1.4)], $\phi(x)=\sum_n c_n\phi(Nx-n)$, or $\hat{\phi}(\xi)=m_0(\xi/N)\hat{\phi}(\xi/N)$, with $m_0(\xi)=N^{-1}\sum_n c_n\,e^{in\xi}$. The different ψ^l can all be written as linear combinations of the $\phi(Nx-n)$. There exist, therefore, trigonometric polynomials m_l so that $\hat{\psi}^l(\xi)=m_l(\xi/N)\hat{\phi}(\xi/N)$ (we assume compact support for ϕ and the ψ^l, so that m_0 and the m_l are indeed polynomials and not infinite series). Orthonormality of the different subspaces in the multiresolution analysis then implies that the $N\times N$ matrix $\mathbb{M}(\xi)$ with entries

$$\mathbb{M}_{lk}(\xi)=m_{l-1}\left(\xi+\frac{2\pi}{N}(k-1)\right)$$

is unitary for all ξ [5]. For $N=2$, this reduces to the standard requirements $m_1(\xi)=e^{i\xi}\overline{m_0(\xi+\pi)}\lambda(\xi)$, with $|\lambda(\xi)|=1$, and $\lambda(\xi+\pi)=\lambda(\xi)$, and $|m_0(\xi)|^2+|m_0(\xi+\pi)|^2=1$. The second condition is [1, eqn. (1.9)] again. If both m_0 and m_1 are trigonometric polynomials, then the only possible choices for $\lambda(\xi)$ are $\lambda(\xi)=\lambda\,e^{ik\xi}$, with $\lambda\in\mathbb{C}$, $|\lambda|=1$ and $k\in\mathbb{Z}$. The simplest choice $\lambda(\xi)\equiv 1$ corresponds to [1, eqn. (1.6)].

For general N, the step of one resolution space V_j to the coarser space V_{j+1} corresponds to a jump of $\log_2 N$ octaves in frequency, since there is a dilation factor N between the two resolutions, and every factor 2 corresponds to one octave. Each of the $N-1$ wavelets ψ^l corresponds therefore to, on average, a bandwidth of

$(N-1)^{-1}\log_2 N$. For $N=4$, for instance, we would have 3 wavelets for 2 octaves, corresponding to an average $\frac{2}{3}$-octave per wavelet, which is better than the 1-octave bandwidth attained by bases with $N=2$.

This naive computation of the average bandwidth of the ψ^l is deceptive, however, as illustrated by the following example. Given an orthonormal wavelet basis with dilation factor 2, the following easy trick generates an orthonormal wavelet basis with dilation factor 4. Let us, for this paragraph only, use a tilde to distinguish the wavelets, spaces in the multiresolution analysis, etc.... for the $N=4$ construction from their counterparts in the $N=2$ case. Define

$$\tilde{m}_0(\xi) = m_0(\xi)m_0(2\xi),$$
$$\tilde{m}_1(\xi) = m_0(\xi)m_1(2\xi),$$
$$\tilde{m}_2(\xi) = m_1(\xi)m_1(2\xi),$$
$$\tilde{m}_3(\xi) = m_1(\xi)m_0(2\xi),$$

where $m_1(\xi) = e^{i\xi}\overline{m_0(\xi+\pi)}$, and $m_0(\xi)$ is the trigonometric polynomial associated with the given orthonormal wavelet basis with $N=2$. Because m_0 satisfies [1, eqn. (1.9)], we easily check that the 4×4 matrix $\tilde{\mathbb{M}}(\xi)$ is indeed unitary for all ξ. The corresponding function $\tilde{\phi}$ is given by

$$\hat{\tilde{\phi}}(\xi) = \prod_{j=1}^{\infty} \tilde{m}_0(4^{-j}\xi) = \prod_{j=1}^{\infty} [m_0(2^{-2j}\xi)m_0(2^{-2j+1}\xi)] = \prod_{j=1}^{\infty} m_0(2^{-j}\xi) = \hat{\phi}(\xi),$$

so that $\tilde{\phi} \equiv \phi$. The scaling spaces $\tilde{V}_j$, spanned by the $\tilde{\phi}(4^{-j}x-k)$, are, therefore, the subsequence of scaling spaces V_m with even index, $\tilde{V}_j = V_{2j}$. The wavelets $\tilde{\psi}^l$, $l=1,2,3$ are given by

$$\hat{\tilde{\psi}}^l(\xi) = \hat{\tilde{m}}_l\left(\frac{\xi}{4}\right)\hat{\phi}\left(\frac{\xi}{4}\right).$$

In particular,

$$\hat{\tilde{\psi}}^1(\xi) = m_1\left(\frac{\xi}{2}\right)m_0\left(\frac{\xi}{4}\right)\hat{\phi}\left(\frac{\xi}{4}\right) = m_1\left(\frac{\xi}{2}\right)\hat{\phi}\left(\frac{\xi}{2}\right) = \hat{\psi}(\xi),$$

or $\tilde{\psi}^1 \equiv \psi$. Since the function ψ is essentially a 1-octave bandwidth function, this shows that the computation above of the average bandwidth of $\frac{2}{3}$-octave for the $\tilde{\psi}^l$ was indeed naive and misleading. The other two wavelets, $\tilde{\psi}^2$, $\tilde{\psi}^3$, are functions not existing in the $N=2$ case, which have in fact better frequency localization. They generate spaces $\tilde{W}_j^2$, $\tilde{W}_j^3$, which together with $\tilde{W}_j^1 = W_{2j}$ complement $\tilde{V}_j = V_{2j}$ to constitute $\tilde{V}_{j-1} = V_{2j-2}$,

$$V_{2j-2} = V_{2j} \oplus W_{2j} \oplus \tilde{W}_j^2 \oplus \tilde{W}_j^3.$$

Since $V_{2j} \oplus W_{2j} = V_{2j-1}$, it follows that $\tilde{W}_j^2 \oplus \tilde{W}_j^3 = W_{2j-1}$. This construction of an $N=4$ multiresolution analysis from an $N=2$ case corresponds therefore to a splitting of all the odd-indexed W_{2j-1} into two spaces, each of approximately $\frac{1}{2}$-octave bandwidth functions, while the even-index W_{2j} remain untouched, and are still generated by 1-octave bandwidth functions.

In the next section we show how to do better than this construction by splitting *every* W_j (as opposed to only the odd-indexed ones) into two parts.

5. Wavelet bases with $\frac{1}{2}$-octave bandwidth wavelets. At the end of the previous section, we had split W_1 into two $\frac{1}{2}$-octave spaces, $\tilde{W}_1^2 \oplus \tilde{W}_1^3$. Dyadic dilations of these spaces are then $\frac{1}{2}$-octave components for any W_m, and these spaces can be used to decompose all of $L^2(\mathbb{R})$. This decomposition can also be derived directly. The key idea

is to start from a conventional multiresolution analysis with dilation factor 2, and to split every space W_j into two $\frac{1}{2}$-octave bandwith subspaces. They key to this splitting is [1, eqn. (1.8)] and the computation leading to [1, eqn. (1.11)]. As shown in [1, § 1], condition [1, (1.8)] ensures that [1, (1.4)] and [1, (1.6)] define an orthonormal basis transform in V_{-1}, from $\{\sqrt{2}\phi(2x-n);\, n\in\mathbb{Z}\}$ to $\{\phi(x-n), \psi(x-n);\, n\in\mathbb{Z}\}$. For the argument to work, it is not essential that the functions appearing in the two sides of [1, (1.4)] are dilated versions of each other. The same argument would work just as well for *any* function f such that the $f(x-k)$ constitute an orthonormal set; with the definitions

$$g_1(x) = 2^{-1/2}\sum_n c_n f(x-n),$$

$$g_2(x) = 2^{-1/2}\sum_n (-1)^n c_{-n+1} f(x-n),$$

the functions $(g_1(x-2n), g_2(x-2m))_{n,m\in\mathbb{Z}}$ are another orthonormal basis for $\overline{\text{Span}\,(f(x-k))}$.

Given α_n satisfying [1, (1.8)], i.e., $\sum_n \alpha_n\alpha_{n+2k} = 2\delta_{k0}$, we can therefore define, for any basic wavelet ψ, the functions $\tilde{\psi}_1$, $\tilde{\psi}_2$ by

$$\begin{aligned}\tilde{\psi}_1(x) &= 2^{-1/2}\sum_n \alpha_n \psi(x-n)\\ \tilde{\psi}_2(x) &= 2^{-1/2}\sum_n (-1)^n \alpha_{-n+1}\psi(x-n);\end{aligned} \tag{2}$$

the functions $\tilde{\psi}_1(x-2n)$, $\tilde{\psi}_2(x-2n)$ then constitute an orthogonal basis for W_0; consequently $(2^{-j/2}\tilde{\psi}_1(2^{-j}x-2n), 2^{-j/2}\tilde{\psi}_2(2^{-j}x-2n);\, j, n\in\mathbb{Z})$ is an orthonormal basis for $L^2(\mathbb{R})$. The Fourier transforms of $\tilde{\psi}_1$, $\tilde{\psi}_2$ will be concentrated on respectively the higher and lower half of the bandwidth of ψ. The bandwidth of $\tilde{\psi}_1$ is, therefore, approximately $\log_2\frac{4}{3} = 2-\log_2 3$ octaves, that of $\tilde{\psi}_2$ approximately $\log_2\frac{3}{2} = \log_2 3 - 1$ octaves. The supportwidth of $\tilde{\psi}_1$, $\tilde{\psi}_2$ will of course be larger than that of ψ.

In Fig. 1 we show two different constructions of $\tilde{\psi}_1$, $\tilde{\psi}_2$, built from two different functions ψ. In each case we have chosen for α_n the same coefficients c_n as used for the definition of ψ (via [1, (1.4)], [1, (1.6)]). We may, of course, also choose different α_n. The support width of $\tilde{\psi}_1$, $\tilde{\psi}_2$ is twice as large as that of ψ. In general, we have

$$\begin{aligned}|\text{support}(\tilde{\psi}_1)| = |\text{support}\,(\tilde{\psi}_2)| &= (\#\text{ of nonzero } \alpha_n) - 1\\ &\quad + (\#\text{ of nonzero } c_n) - 1.\end{aligned}$$

For the choice $\alpha_n = c_n$ made in Fig. 1, we have, therefore,

$$|\text{support}\,(\tilde{\psi}_1)| = |\text{support}\,(\tilde{\psi}_2)| = 2|\text{support}\,(\psi)|.$$

Note that with the choice $\alpha_n = c_n$ the two wavelets constructed here are (up to dilation) exactly the two "new" wavelets constructed in the previous section.

The plots of $|\hat{\tilde{\psi}}_1|$, $|\hat{\tilde{\psi}}_2|$ in Fig. 1 have "side-lobes" that make the splitting less than perfect. Such side-lobes are unavoidable. We have

$$\hat{\tilde{\psi}}_1(\xi) = a(\xi)\hat{\psi}(\xi), \qquad \hat{\tilde{\psi}}_2(\xi) = e^{i\xi}\overline{a(\xi+\pi)}\hat{\psi}(\xi),$$

with $a(\xi) = 2^{-1/2}\sum_n \alpha_n e^{in\xi}$. Condition [1, (1.8)] implies $|a(\xi)|^2 + |a(\xi+\pi)|^2 = 2$. For small $|\xi| \leqq \xi_0$ we have $|\hat{\tilde{\psi}}_1| \simeq \sqrt{2}|\hat{\psi}|$, or $|a(\xi)| \simeq \sqrt{2}$. Consequently, $|a(\xi+\pi)| \simeq 0$ for $|\xi| \leqq \xi_0$. Since a is periodic, this implies $|a(\xi+\pi)| \simeq 0$ for $|\xi - 2\pi| \leqq \xi_0$, or $|a(\xi)| \simeq \sqrt{2}$, hence $|\hat{\tilde{\psi}}_1| \simeq \sqrt{2}|\hat{\psi}|$ in this region also. This causes the "side-lobes" on the figure. The only way to reduce them is to start from ψ with very concentrated Fourier transform

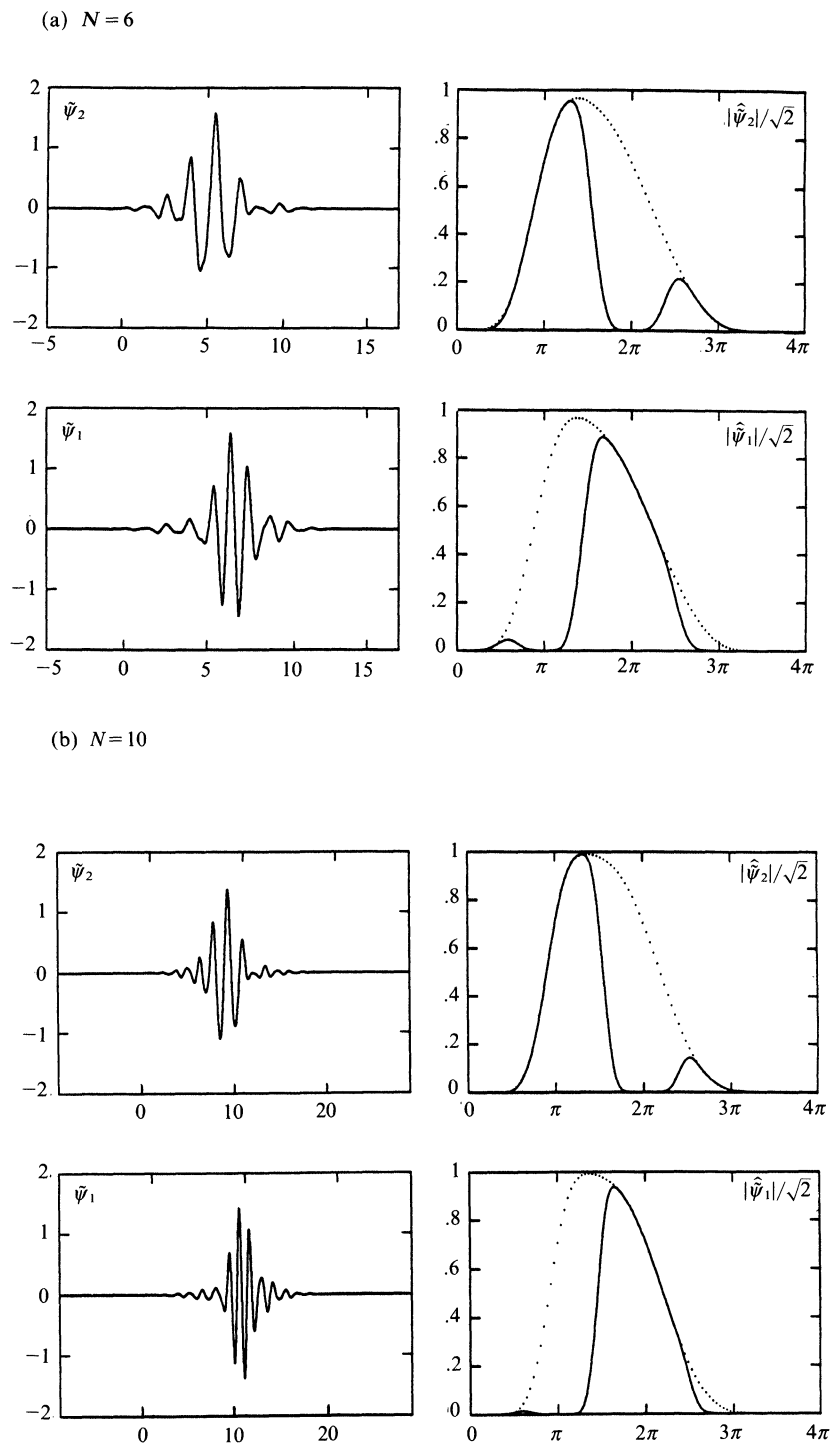

FIG. 1. *Graphs of the "$\frac{1}{2}$-octave bandwidth" functions $\tilde{\psi}_1$, $\tilde{\psi}_2$ and the absolute values of their Fourier transforms $|\hat{\tilde{\psi}}_1|$, $|\hat{\tilde{\psi}}_2|$. The dotted line in each case is the graph of $|\hat{\psi}|$. We have $2|\hat{\psi}|^2 = |\hat{\tilde{\psi}}_1|^2 + |\hat{\tilde{\psi}}_2|^2$. (This is clearly illustrated by the graphs. Note that we have plotted $|\hat{\tilde{\psi}}_1|/\sqrt{2}$ and $|\hat{\tilde{\psi}}_2|/\sqrt{2}$ in order to make the comparison with $|\hat{\psi}|$.) In both cases the α_n (see (2)) are the same as the coefficients c_n from which ψ is defined; the function ψ in these two examples corresponds to* (a) *the case $N=6$ in* [1, § 2] *and* (b) *the case $N=10$ in* [1, § 2].

$|\hat{\psi}|$. This is why the effect becomes less pronounced as N increases. (The Fourier transform $|\hat{\psi}|$ becomes more concentrated as N increases; see Fig. 7 in [2].)

Remarks.

(1) In case even better frequency localization is desired, this splitting trick can be repeated: we can replace ψ by $2j$ functions, each corresponding to a 2^{-j}-octave bandwidth, and which have to be translated by integer multiples of 2^j,

$$\overline{\text{Span}\,\{\psi(x-n)\}} = \overline{\text{Span}\,\{\tilde{\psi}_l(x-2^j m);\ l=1,\dots,2^j,\ m\in\mathbb{Z}\}}.$$

At every splitting, the "side-lobe effect" takes its toll, however, marring the frequency localization; see [8].

(2) The functions $\tilde{\psi}_1$, $\tilde{\psi}_2$ constructed are special cases of the "wavelet packets" discovered by Coifman and Meyer [6], which in one framework encompass many different choices of orthonormal bases, of which the wavelet is one extreme example. Another extreme within the same framework is a basis closer in spirit to the windowed Fourier transform; infinitely many intermediate choices are possible; see [9] for applications.

6. Multidimensional "splitting." The "splitting trick" also allows selective splitting in higher-dimensional multiresolution analysis. For the sake of simplicity we restrict ourselves to two dimensions. A standard way of generating a two-dimensional wavelet basis from a one-dimensional multiresolution analysis is to define [7]

$$\begin{aligned}\Phi(x,y) &= \phi(x)\phi(y),\\ \Psi^1(x,y) &= \psi(x)\phi(y),\\ \Psi^2(x,y) &= \phi(x)\psi(y),\\ \Psi^3(x,y) &= \psi(x)\psi(y).\end{aligned} \tag{3}$$

The orthonormal basis of wavelets is then given by the $\Psi^l_{j,k}$, with $l=1,2,3$, $j\in\mathbb{Z}$ and $k=(k_1,k_2)\in\mathbb{Z}^2$ defined by

$$\Psi^l_{j,k}(x,y) = 2^{-j}\Psi^l(2^{-j}x-k_1, 2^{-j}y-k_2).$$

A good way to visualize what this construction means is to look at it in the Fourier plane for the special choice $\hat{\phi}(\xi) = (2\pi)^{-1/2}$ if $|\xi|\leqq\pi$, 0 otherwise, and the corresponding $\hat{\psi}(\xi) = (2\pi)^{-1/2}$ if $\pi<|\xi|\leqq 2\pi$, 0 otherwise. We easily check that for this choice the space V_j is exactly $L^2([-2^{-j}\pi, 2^{-j}\pi])$, and $W_j = L^2([-2^{-j+1}\pi, -2^{-j}\pi]\cup[2^{-j}\pi, 2^{-j+1}\pi])$, so that the whole ladder of one-dimensional multiresolution spaces can be simply represented by the supports of the corresponding functions. Of course, these particular ϕ and ψ decay too slowly to be useful in practice, but the visualization they lead to in Fourier space is still "morally true" for other, more useful choices, even though the splitting is not as clean cut. The two-dimensional multiresolution spaces $\mathbf{V}_j$, and their complement spaces $\mathbf{W}^l_j$, generated by (3) can also be written

$$\begin{aligned}\mathbf{V}_j &= V_j\otimes V_j,\\ \mathbf{W}^1_j &= W_j\otimes V_j,\\ \mathbf{W}^2_j &= V_j\otimes W_j,\\ \mathbf{W}^3_j &= W_j\otimes W_j.\end{aligned}$$

For the special choices of ϕ, ψ described above, these two-dimensional spaces are again L^2-spaces of particular domains carved out in the Fourier plane. For instance, $\mathbf{V}_j = L^2([-2^{-j}\pi, 2^{-j}\pi]) \otimes L^2([-2^{-j}\pi, 2^{-j}\pi]) = L^2([-2^{-j}\pi, 2^{-j}\pi] \times [-2^{-j}\pi, 2^{-j}\pi])$; in particular, $\mathbf{V}_0 = L^2([-\pi, \pi]^2)$. For every j, the sum $\mathbf{W}_j^1 \oplus \mathbf{W}_j^2 \oplus \mathbf{W}_j^3$ is the orthogonal complement in $\mathbf{V}_{j-1}$ of $\mathbf{V}_j$, which corresponds to the annulus $[-2^{-j+1}\pi, 2^{-j+1}\pi]^2 \backslash [-2^{-j}\pi, 2^{-j}\pi]^2$. All this is visualized in Fig. 2(a): the small central square corresponds to (say) $\mathbf{V}_0$; adding to it the two vertical rectangles corresponding to $\mathbf{W}_0^1$, the two horizontal rectangles for $\mathbf{W}_0^2$, and the four corner squares for $\mathbf{W}_0^3$ lead to the bigger square representing $\mathbf{V}_{-1}$. The structure then repeats in the next annulus, to constitute $\mathbf{V}_{-2}$. The angular resolution in the Fourier plane of this scheme is not very good, as shown by the figure. Figure 2(b) shows what the same two-dimensional construction looks like when we start from a one-dimensional multiresolution analysis with dilation factor 4, as given in § 4. In this case the one-dimensional scheme has already three wavelets,

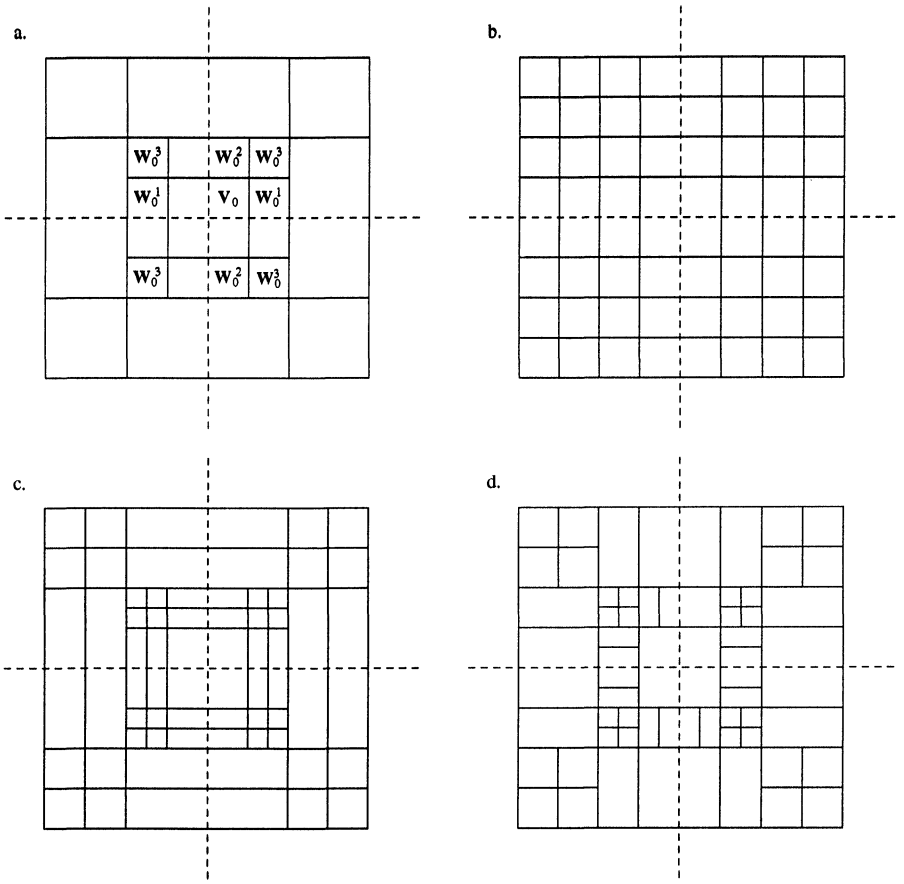

FIG. 2. *Visualization of the localization in the Fourier plane achieved by various two-dimensional multiresolution schemes*:

(a) *the standard product scheme starting from a one-dimensional analysis with dilation factor* 2,

(b) *product scheme from a one-dimensional analysis with dilation factor* 4, *derived from a multiresolution analysis with factor* 2 *as in* § 4,

(c) *product scheme from a one-dimensional analysis with two* $\frac{1}{2}$*-octave bandwidth wavelets rather than one* 1*-octave bandwidth wavelet,*

(d) *a nonproduct scheme obtained by the "splitting trick."*

so that the two-dimensional product scheme ends up with $2\times 3+3^2=15$ wavelets. Figure 2(b) represents one step (with dilation 4) in the multiresolution scale, as compared to two steps (with dilation factor 2), i.e., two successive annuli in Fig. 2(a). The central part of the two pictures is identical; the only difference between the two pictures is that the outer annulus of Fig. 2(a) is split into many pieces to give Fig. 2(b), while the inner annulus is untouched. This corresponds to the "splitting of one level out of two" shown at the end of § 4. The result is good angular resolution for some wavelets (corresponding to the outer layer in Fig. 2(b)), bad for others (corresponding to the most central rectangles in Fig. 2(b)).

Figure 2(c) shows the same picture again, with two steps in a multiresolution analysis with dilation factor 2, but for a product structure of type (3) starting from the two $\frac{1}{2}$-octave bandwidth wavelets constructed in § 5, rather than the 1-octave bandwidth wavelet ψ. The scaling function Φ is the same, but there are now $2\times 2+2^2=8$ wavelets (as opposed to 3 for Fig. 2(a), and 15 for Fig. 2(b)). Figure 2(c) can be obtained from Fig. 2(a) by splitting every annulus (inner as well as outer) into halves by cuts in both horizontal and vertical directions. This improves the angular resolution on the squares in the corners (corresponding to the $\mathbf{W}_j^3$ of Fig. 2(a), but does nothing for the angular resolution of the rectangles (corresponding to $\mathbf{W}_j^2$ or $\mathbf{W}_j^1$ in Fig. 2(a)), which were split better in the outer annulus of Fig. 2(b). The best angular resolution can be obtained by giving up a product structure analogous to (3) and just carving up every one of the $\mathbf{W}_j^l$ spaces of Fig. 2(a) vertically and/or horizontally, by applying the "splitting trick" in x and/or y, until the desired resolution is achieved. An example is given in Fig. 2(d). This still corresponds to an orthonormal basis, and to a fast algorithm for decomposing and reconstructing functions, as described in [1, § 1], although the organization is somewhat more complex. If even better angular resolution is required, then we can repeat the splitting trick as many times as necessary.

Acknowledgment. I. Daubechies would like to thank Professor Y. Meyer and the University of Paris IX for inviting her and for their hospitality.

REFERENCES

[1] I. DAUBECHIES, *Orthonormal bases of compactly supported wavelets* II. *Variations on a theme*, SIAM J. Math. Anal., this issue (1993), pp. 499–519.

[2] ———, *Orthonormal bases of compactly supported wavelets*, Comm. Pure Appl. Math., 41 (1988), pp. 909–996.

[3] Y. MEYER, *Principe d'incertitude, bases hilbertiennes et algèbres d'opérateurs.* Sém. Bourbaki, 662, 1985–1986.

[4] C. DORIZE AND K. GRAM-HANSEN, *Wavelet decomposition in the field of time-frequency analysis*, Conference on Wavelets, Marseille, France, June 1989.

[5] P. AUSCHER, *Ondelettes fractales et applications*, Ph.D. thesis, CEREMADE, University of Paris IX, Paris, France, 1989.

[6] R. COIFMAN AND MEYER, *Orthonormal Wavelet Packet Bases*, Yale University, New Haven, CT, preprint, 1990.

[7] S. MALLAT, *A theory for multiresolution signal decomposition: the wavelet representation*, IEEE Trans. on Pattern Analysis and Machine Intelligence, 11 (1989), pp. 674–693.

[8] R. COIFMAN, Y. MEYER, AND V. WICKERHAUSER, *Size properties of wavelet packets*, in Wavelets and their Applications, M. B. Ruskai et al., eds., Jones and Bartlett, Boston, MA, 1992, pp. 453–470.

[9] R. COIFMAN AND V. WICKERHAUSER, *Entropy-based algorithms for best basis selection*, IEEE Trans. Inform. Theory, 38 (1992), pp. 713–718.

[10] K. KOVAČEVIĆ AND M. VETTERLI, *Perfect reconstruction filter banks with rational sampling rates*, Columbia Univ., New York, preprint, 1991; IEEE Trans. Signal Processing, submitted.